THE JOURNAL OF BIOLOGICAL CHEMISTRY VOL. 283, NO. 2, pp. 766–773, January 11, 2008
Printed in the U.S.A.

Kinetics of ADP Dissociation from the Trail and Lead Heads of Actomyosin V following the Power Stroke*

Received for publication, May 25, 2007, and in revised form, October 17, 2007 Published, JBC Papers in Press, October 27, 2007, DOI 10.1074/jbc.M704313200

Eva Forgacs[‡1], Suzanne Cartwright[‡], Takeshi Sakamoto[§2], James R. Sellers[§], John E. T. Corrie[¶3], Martin R. Webb[¶3], and Howard D. White[‡4]

From the [‡]Department of Physiological Sciences, Eastern Virginia Medical School, Norfolk, Virginia 23507, [¶]Medical Research Council National Institute for Medical Research, Mill Hill, London NW7 1AA, United Kingdom, and the [§]Laboratory of Molecular Physiology, NHLBI, National Institutes of Health, Bethesda, Maryland 20892

Myosin V is a cellular motor protein, which transports cargos along actin filaments. It moves processively by 36-nm steps that require at least one of the two heads to be tightly bound to actin throughout the catalytic cycle. To elucidate the kinetic mechanism of processivity, we measured the rate of product release from the double-headed myosin V-HMM using a new ATP analogue, 3′-(7-diethylaminocoumarin-3-carbonylamino)-3′-deoxy-ATP (deac-aminoATP), which undergoes a 20-fold increase in fluorescence emission intensity when bound to the active site of myosin V (Forgacs, E., Cartwright, S., Kovács, M., Sakamoto, T., Sellers, J. R., Corrie, J. E. T., Webb, M. R., and White, H. D. (2006) *Biochemistry* 45, 13035–13045). The kinetics of ADP and deac-aminoADP dissociation from actomyosin V-HMM, following the power stroke, were determined using double-mixing stopped-flow fluorescence. These used either deac-aminoATP as the substrate with ADP or ATP chase or alternatively ATP as the substrate with either a deac-aminoADP or deac-aminoATP chase. Both sets of experiments show that the observed rate of ADP or deac-aminoADP dissociation from the trail head of actomyosin V-HMM is the same as from actomyosin V-S1. The dissociation of ADP from the lead head is decreased by up to 250-fold.

Myosin V is an unconventional myosin that transports organelles such as vesicles in neurons and melanosomes in melanocytes along actin tracks (1). To do this, myosin V has evolved the ability to move processively on actin for several μm, requiring many ATP hydrolysis cycles (2). The processivity is at least partially explained by a kinetic mechanism in which the slow rate of ADP dissociation is the rate-limiting step of ATP hydrolysis (3, 4).

This is in contrast to the myosin II mechanism, in which ADP dissociation is much faster and dissociation of actin from myosin occurs with each cycle of ATP hydrolysis. As a result, myosin V has a much higher duty cycle, and even single headed myosin V is in the strongly bound actomyosin-ADP state 80–90% of the time during steady-state hydrolysis (3). It has also been suggested that additional mechanisms promoting processivity may involve gating of product release (5, 6). Thus, biochemical cycles of the lead and trail head keep out of synchrony, so one head of the molecule is always strongly attached (actomyosin or actomyosin-ADP). Biochemical (7), mechanical (5, 6, 8), and structural studies (9, 10) suggest that intramolecular strain accelerates ADP dissociation from the trail head and/or inhibits ADP dissociation from the lead head. The long lever arm of myosin V, which contains six calmodulin or light chain molecules, produces a 20–25-nm power stroke that can be observed as two substeps of 15–20 and 5 nm (11, 12).

Biochemical evidence showing the interaction between the two heads is from kinetic data obtained by Rosenfeld and Sweeney (7), who observed biphasic dissociation of mdADP[5] from actomyosin V-HMM. In these single-mixing stopped-flow experiments, the rates of mdADP dissociation were measured by mixing myosin-mdADP complexes with actin in the presence of either a large excess of ATP or ADP that can act as a chase reagent, binding to nucleotide-free sites as they form. An alternative approach to measure the post-power stroke dissociation of ADP resulting from a single turnover of ATP hydrolysis is to use double-mixing stopped-flow measurements. In these experiments, the myosin is first mixed with ATP (or fluorescent analogues), incubated for a few seconds to allow the ATP to bind to the myosin and be hydrolyzed, and then mixed with actin. A power stroke is associated with P_i dissociation from actomyosin-ADP-P_i but is not produced by either apomyosin or myosin-ADP binding to actin (13). Thus, double-mixing experiments are required to determine the kinetics of product dissociation following a power stroke. Double mixing experiments have previously only been done in the presence of an ATP chase (7). In these experiments, the ATP chase rapidly binds to the trail head and dissociates it from actin. Thus, the kinetics of mdADP release from the lead head, while the molecule remains under the strain produced by a

* This work was supported by National Institutes of Health Grant EB00209 and a grant from the Carman Foundation. The costs of publication of this article were defrayed in part by the payment of page charges. This article must therefore be hereby marked "*advertisement*" in accordance with 18 U.S.C. Section 1734 solely to indicate this fact.
[1] Supported by an American Heart Association postdoctoral fellowship.
[2] Supported by a Japanese Society for the Promotion of Science Fellowship.
[3] Supported by the United Kingdom Medical Research Council.
[4] To whom correspondence should be addressed. Tel.: 757-446-5652; Fax: 757-624-2270; E-mail: whitehd@evms.edu.

[5] The abbreviations used are: mdADP, 3′-*O*-(*N*-methylanthraniloyl)-2′-deoxyadenosine 5′-diphosphate; mdATP, 3′-*O*-(*N*-methylanthraniloyl)-2′-deoxyadenosine 5′-triphosphate; actin, filamentous actin; myosin V-S1, myosin V subfragment 1; myosin V-HMM, myosin V heavy meromyosin; deac-aminoATP, 3′-(7-diethylaminocoumarin-3-carbonylamino)-3′-deoxyadenosine 5′-triphosphate; deac-aminoADP, 3′-(7-diethylaminocoumarin-3-carbonylamino)-3′-deoxyadenosine 5′-diphosphate; TIRF, total internal reflectance fluorescence; MOPS, 4-morpholinepropanesulfonic acid.

power stroke, was not determined. An additional complication of using mdATP as the fluorescent substrate in these experiments is that ~70% of the fluorescence signal is associated with phosphate dissociation, and only ~30% is associated with the dissociation of mdADP from actomyosin V-mdADP-P_i (7). Although the rate of P_i dissociation is at least 10-fold more rapid than mdADP dissociation from actomyosin V, the relatively small amplitude associated with mdADP release and the temporal overlap between the two processes complicate the kinetic analysis. We made an initial study of product dissociation by double-mixing experiments using mdATP as a substrate with an ADP chase but did not observe a significant difference between the kinetics of product dissociation from actomyosin V-HMM-mdADP-P_i and actomyosin V-S1-mdADP-P_i (15).

We therefore utilized the fluorescent ATP analogue, deac-aminoATP, to study the kinetics of the nucleoside diphosphate dissociation steps. A ~20-fold fluorescence increase is observed when deac-aminoATP binds to myosin V-S1, and >95% of the fluorescence change upon product dissociation is associated with deac-aminoADP dissociation from actomyosin V-S1 (16). Based on these studies, we carried out a series of double-mixing stopped-flow experiments to measure ADP and deac-aminoADP dissociation from the double-headed complexes of actomyosin V-HMM-deac-aminoADP-P_i and actomyosin V-HMM-ADP-P_i. Single molecule total internal reflectance fluorescence (TIRF) experiments were also done with deac-aminoATP to demonstrate that this substrate supports processive movement of myosin V on actin.

EXPERIMENTAL PROCEDURES

Preparations of Myosin V—Mouse myosin V-HMM and myosin V-S1 were co-expressed with calmodulin in a baculovirus/Sf9 cell system and purified using FLAG affinity chromatography (17) and then concentrated and fractionated on a MonoQ ion exchange column with a linear gradient of 0.1–0.5 M KCl. The concentration of myosin V-HMM active sites was determined from $A_{280} - 1.5A_{320}$ (A_{320} was subtracted to correct for light scattering) and $\epsilon_{\mu M} = 0.123\ cm^{-1}$, calculated from the number of tyrosine and tryptophan residues and their subunit molar extinction coefficients at 280 nm: $\epsilon_M = (n = 10)_{Trp} \times 5690 + (n = 52)_{Tyr} \times 1280$ (18). All preparations were analyzed by SDS protein gel electrophoresis and by active site titration with deac-aminoATP. Myosin V-HMM and myosin V-S1 were stored on ice in buffer containing 10 mM MOPS, 3 mM $MgCl_2$, 1 mM EGTA, and 400 mM KCl, pH 7.5, and used within 72 h.

Reagents—Actin was purified from rabbit skeletal muscle (19). ATP and ADP were purchased from Sigma. *N*-Methylanthraniloyl derivatives of 2′-deoxyADP (mdADP) and ATP (mdATP) were synthesized and purified according to the method of Hiratsuka (20). Deac-aminoATP and deac-aminoADP were synthesized by the method of Webb *et al.* (21). Deac-aminonucleotide concentrations were based upon molar extinction coefficients of the deac-aminoATP and deac-aminoADP, $\epsilon_{429} = 46{,}800\ M^{-1}\ cm^{-1}$.

Stopped-flow Experiments—All stopped-flow measurements were done at 20 °C using an SF-2001 stopped-flow apparatus (KinTek Corp., Austin, TX) fitted with two 2-ml and one 5-ml syringe. The excitation light from a 75-watt xenon lamp was selected by using a 0.125-m monochromator (PTI, South Brunswick, NJ). Deac-aminoATP and deac-aminoADP were excited at 430 nm, and the emitted light was selected using a 450-nm long pass filter. In mdATP experiments, excitation was at 360 nm, and emission was selected using a 400-nm-long pass filter. Stocks of myosin V-HMM and myosin V-S1 were diluted from buffer containing 400 mM KCl to obtain the desired protein concentration and a final KCl concentration of 112 mM just prior to use. Myosin V was mixed with ATP or deac-aminoATP in buffer containing no KCl, incubated for the required time, and then mixed with actin containing the desired nucleotide chase (also in buffer with no KCl). The final concentration of buffer in the flow cell was 10 mM MOPS, pH 7.5, 3 mM $MgCl_2$, 25 mM KCl, and 1 mM EGTA. Actin filaments were stabilized with equimolar phalloidin. Actin (80 μM) was treated for 1 h with either 0.01 unit of apyrase for experiments used without a chase to hydrolyze traces of ADP or ATP. Stock solutions of actin (80 μM) and ADP (2 mM) were treated for 1 h at 20 °C with 1 mM glucose and 0.01 unit/ml hexokinase to remove traces of ATP in experiments where the actin contained an ADP chase.

TIRF Assay—The TIRF assay was performed as described previously (22).

Data Analysis and Kinetic Simulation—Three to four data traces of 500 points were averaged, and the observed rate constants were obtained by fitting the data to one, two, or three exponential terms using the software package included with the Kintek stopped-flow instrument and using nonlinear least squares routines in the Scientist package (23). In all cases, the amplitudes and rate constants obtained using the two software packages agreed to within 1–2%. Fitting data to two or more exponential terms is robust and will determine a unique set of rate and amplitude terms if the rate constants differ by a factor of more than 5-fold. The smallest difference between the rate constants was in Fig. 1, where there was a 7-fold difference between the two fastest terms. The time dependence of the fluorescence was collected and fit *versus* log time because of the large range over which changes in fluorescence were observed and because it allows much better scrutiny of the quality of the fit than with linear plots that are customarily used. A log time base is also preferable for multiexponential fits, because the same weighting is given to each of the exponential terms, whereas the fitting with a linear time base gives heavier weighting to the slower processes.

RESULTS

Initial Studies of the Rates of Product Dissociation from Actomyosin V-HMM-mdADP-P_i—In our initial studies, we used mdATP to determine the kinetics of product dissociation from the actomyosin V-HMM-mdADP-P_i complex (Fig. 1). Myosin V-HMM was first mixed with mdATP and then actin containing either no chase or an ATP or ADP chase in single-turnover double-mixing stopped-flow experiments. The data were not normalized but have been displaced vertically so that they do not overlap each other. Although the total amplitudes were the same within experimental error, the fit amplitudes were normalized to a total of 1.0 to make comparison easier. For all three

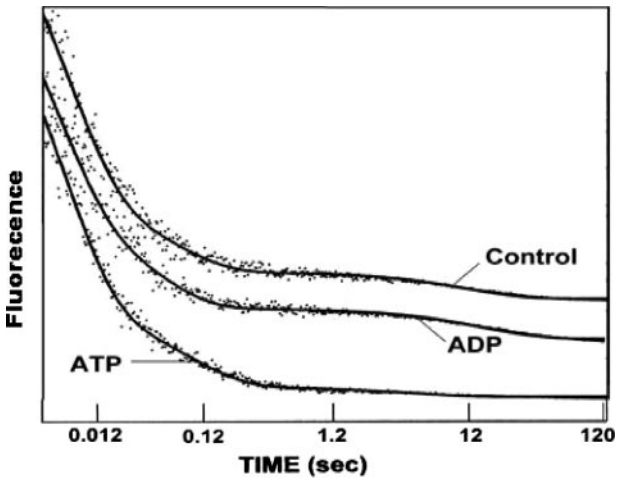

FIGURE 1. **Product dissociation from actomyosin V-HMM-mdADP-P_i.** Myosin V-HMM (0.3 μM sites) was mixed at 20 °C with 0.3 μM mdATP, held in a delay line for 20 s, and then mixed with 20 μM actin and either a 200 μM ADP chase, a 200 μM ATP chase, or no chase. The data were fit to the sum of three exponentials: $I(t) = I_1e^{-k1t} + I_2e^{-k2t} + I_3e^{-k3t}$; no chase: $I_1 = 0.77$, $k_1 = 75\ s^{-1}$, $I_2 = 0.155$, $k_2 = 9.0\ s^{-1}$, $I_3 = 0.078$, $k_3 = 0.03\ s^{-1}$; ADP chase: $I_1 = 0.77$, $k_1 = 67\ s^{-1}$, $I_2 = 0.155$, $k_2 = 10.1\ s^{-1}$, $I_3 = 0.078$, $k_3 = 0.03\ s^{-1}$; ATP chase: $I_1 = 0.74$, $k_1 = 73\ s^{-1}$, $I_2 = 0.25$, $k_2 = 10.8\ s^{-1}$.

experiments, there was a fast and large (65–70% of total amplitude) fluorescence decrease at a rate of ~75 s^{-1}, k_{obs1}, which is similar to the rate of P_i dissociation (7), and a smaller amplitude (25–30%) fluorescence decrease at ~10 s^{-1} (k_{obs2}), assigned to mdADP dissociation. When an ADP chase (or no chase) was used, a third small amplitude phase was also observed (5–6%) with a rate constant of ~0.03 s^{-1} (k_{obs3}). With an ATP chase, the rates and amplitudes on the two fast phases were similar to those observed with no chase or with an ADP chase, but the amplitude of the slowest component, 0.03 s^{-1}, was less than 1%, and the data were fit equally well by two exponential terms. However, because the amplitude of the slowest component (k_{obs3}) with no nucleotide chase or with an ADP chase was significantly (3–4-fold) lower than that of k_{obs2}, we were not certain of its significance. Based on our observations and those of Rosenfeld and Sweeney (7), it became apparent that mdATP is not the ideal substrate with which to study the kinetics of ADP dissociation from actomyosin V-ADP-P_i, as discussed in the Introduction. We therefore decided to utilize deac-aminoATP for this work, because it has several features that make it preferable to mdATP for these studies (16). 1) Deac-amino nucleotides have a much larger increase in fluorescence emission (~20-fold upon binding to myosin V), which provides a much better signal/noise ratio than mdATP and a useable signal with as little as 10 nM nucleotide in the final reaction mix. This also allows deac-amino nucleotides to be used in chase experiments at ratios as high as 100 times the active site concentration with a good signal to noise ratio. 2) Single turnover experiments of myosin V-S1 with deac-aminoATP indicated that >95% of the fluorescence enhancement remains after dissociation of P_i from the active site of myosin V, and, therefore, the fluorescence change is specific for deac-aminoADP dissociation (7).

Deac-aminoATP Binding to Myosin V-HMM (Active Site Titration)—We have conducted single-turnover stopped-flow active-site titrations of myosin V-HMM similar to those previously reported for myosin V-S1 (16) to determine the kinetics of myosin V hydrolysis of deac-aminoATP and active site concentrations of the myosin V-HMM (data not shown). The active site concentration determined in this manner for myosin V-HMM was 95–100% of that determined from A_{280} using the calculated extinction coefficient of myosin V-HMM. It is important that a high percentage of the protein be catalytically active when measuring properties of a dimeric protein, because one inactive head will influence the function of the whole molecule (24). The observed rate constants for deac-aminoATP binding, steady state hydrolysis, and deac-aminoADP affinity to myosin V-HMM are similar to those previously measured with myosin V-S1, which provides evidence that the two heads of myosin V-HMM function independently in the absence of actin (Table 1).

TABLE 1
Rate constants of deac-aminoATP binding and hydrolysis by myosin V-HMM and myosin V-S1 determined from single turnover experiments

$$M + T \xrightarrow{k_T} M\text{-}T \leftrightarrow M\text{-}D\text{-}P \xrightarrow{k_{ss}} M\text{-}D \xrightarrow{1/K_D} M$$

where M represents myosin V-S1 or myosin V-HMM, T is deac-aminoATP, D is deac-aminoADP, and P is inorganic phosphate. Data for S1 are from Forgacs *et al.* (16). Experimental conditions were as follows: 10 mM MOPS, 25 mM KCl, 3 mM $MgCl_2$, 1 mM EGTA, pH 7.5, 20 °C.

	k_T	k_{ss}	$1/K_D$
	$\mu M^{-1}\ s^{-1}$	s^{-1}	μM
HMM	3.5 ± 0.03	0.027 ± 0.03	0.07 ± 0.02
S1	3.4 ± 0.03	0.025 ± 0.02	0.09 ± 0.02

Kinetics of Product Dissociation from Actomyosin V-HMM-deac-aminoADP-P_i—We have carried out double mixing stopped-flow experiments to determine the rates of product dissociation utilizing deac-aminoATP as the substrate (Fig. 2). Equimolar amounts of myosin V-HMM and deac-aminoATP were mixed and aged in a delay line for 20 s. The solution was then mixed either with actin alone (treated with apyrase to ensure that there was no free nucleotide present) or with actin plus an ADP or ATP chase. When an ADP chase was used, we observed two distinct phases with rate constants of 0.46 s^{-1} for the faster and 0.015 s^{-1} for the slower phase (Fig. 2*A*). There was no actin dependence of either the slow or fast rates (Fig. 2*B*), as would be expected based on the rapid ($2 \times 10^7\ M^{-1}\ s^{-1}$) second-order rate constant of myosin V-S1-deac-amino-ADP-P_i binding to actin (16), and slow and fast phases were fit to maximum rates of 0.48 ± 0.01 and 0.015 ± 0.002 s^{-1}. The amplitudes associated with the slow phase in Figs. 2*A* and 3*A* are 40–45% of the total amplitude, which is close to the 50% expected for nucleotide dissociation from one of the two heads. Moreover, the slow phase is eliminated by the presence of calcium (data not shown), which has been shown to dissociate one or more of the calmodulin light chains from the myosin V lever arm and would be expected to interfere with the transmission of strain between the two heads.

The rate of the faster component of deac-aminoADP dissociation from actomyosin V-HMM-deac-aminoADP-P_i is the same as that observed for actomyosin V-S1-deac-aminoADP-P_i, 0.48 s^{-1} (Fig. 2*C*), and the rate of the slower component is 32 times less. In contrast to experiments with an ADP chase, the

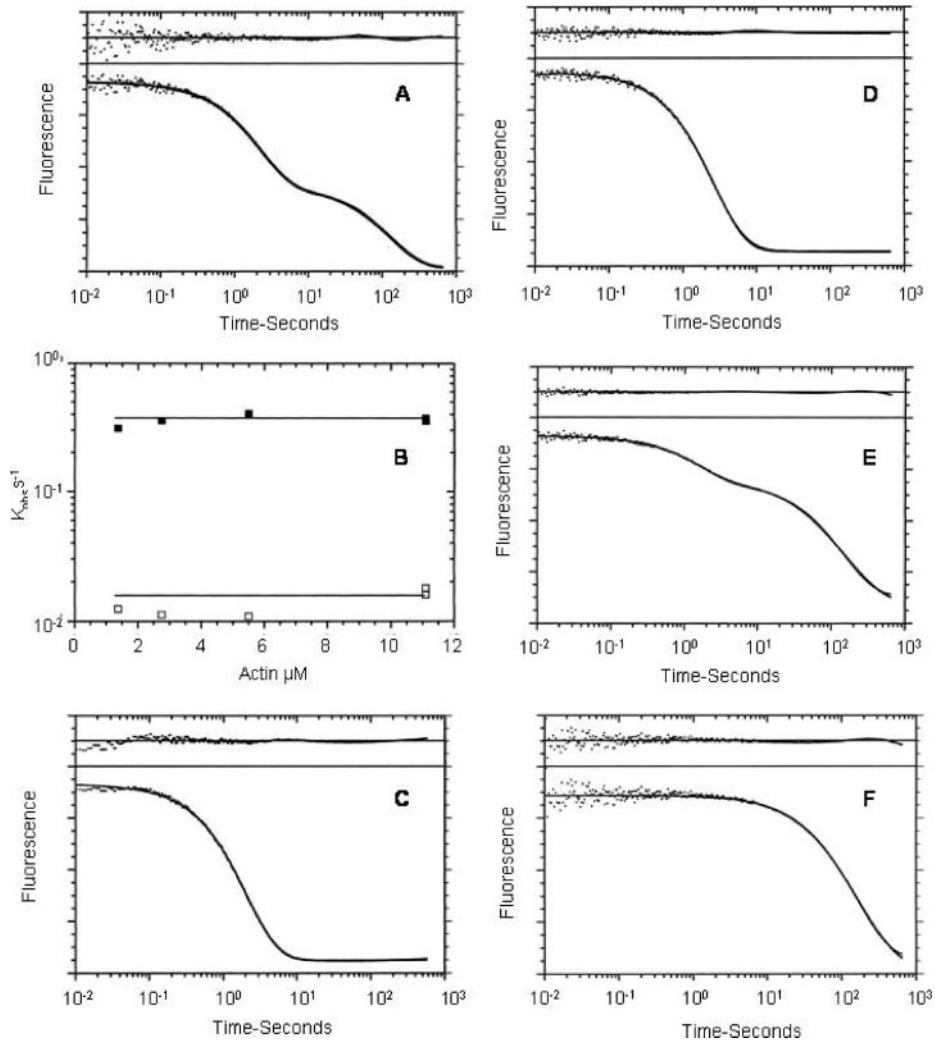

FIGURE 2. **Kinetics of product dissociation from actomyosin V-deac-aminoADP-P_i.** *A*, 0.25 μM myosin V-HMM was mixed with 0.25 μM deac-aminoATP, held 20 s in a delay line, and then mixed with 20 μM phalloidin-actin and 200 μM ADP. The *solid line* through the data is $I(t) = 0.403e^{-0.46t} + 0.313e^{-0.015t} + C$. *B*, actin dependence of the fast and slow components of deac-aminoADP dissociation from actomyosin V-HMM-deac-aminoADP-P_i. The experiments were similar to those in *A*, except that the actin concentration was varied as indicated. The *lines* through the data are for rate constants of 0.48 ± 0.01 and 0.015 ± 0.002 s^{-1}. *C*, 0.25 μM myosin V-S1 was mixed with 0.25 μM deac-aminoATP, held 20 s in a delay line, and then mixed with 20 μM phalloidin-actin and 200 μM ADP. The *solid line* through the data is $I(t) = 0.86\ e^{-0.48t} + C$. *D*, 0.25 μM myosin V-HMM was mixed with 0.25 μM deac-aminoATP, held 20 s in a delay line, and then mixed with 20 μM phalloidin-actin and 200 μM ATP. The *solid line* through the data is $I(t) = 0.87e^{-0.37t} + C$. *E*, 0.25 μM myosin V-HMM was mixed with 0.25 μM deac-aminoATP, held 20 s in a delay line, and then mixed with 20 μM phalloidin-actin (apyrase-treated). The *solid line* through the data is $I(t) = 0.18e^{-0.58t} + 0.44e^{-0.0068t} + C$. *F*, 0.25 μM myosin V-HMM was mixed with 0.06 μM deac-aminoATP, held 20 s in a delay line, and then mixed with 20 μM phalloidin-actin (apyrase-treated). The *solid line* through the data is $I(t) = 0.12e^{-0.006t} + C$.

rate of deac-aminoADP dissociation measured in a double-mixing experiment with an ATP chase is fit well with a slower single rate constant of 0.37 s^{-1} (Fig. 2*D*). Modeling a mechanism of two consecutive reactions at 0.48 s^{-1} predicts a fluorescence signal that is very close to a single exponential with a rate constant that is 0.65 times that of the individual molecular rate constants, ~0.32 s^{-1}, which is in reasonably good agreement with the observed rate of 0.37 s^{-1}.

In the absence of a chase (apyrase-treated actin), the kinetics of deac-aminoADP dissociation from actomyosin V-HMM-deac-aminoADP-P_i are fit by two rate constants of 0.58 and 0.0068 s^{-1} (Fig. 2*E*). The apparently more rapid rate of the fast component and its smaller amplitude are expected because, in the absence of a chase, the deac-aminoADP does not completely dissociate from the active site. The final deac-aminoADP concentration, 0.07 μM, is similar to the dissociation constant of deac-aminoADP from actomyosin V-S1, 0.09 μM. The observed rate of dissociation is the sum of the forward and reverse rates of deac-aminoADP binding. The rate of the slow component is reduced by a factor of 2 in the absence of a chase. This is a measure of the effect of ADP bound to one head upon the rate of deac-aminoADP dissociation from the second head. Additional evidence for this interpretation is provided by experiments in which the concentration of deac-aminoATP in the first mix was reduced to 0.25 of the active site concentration. Under these conditions, it would be expected that if binding of substrate to the heads is statistically random, 37% of the molecules would have products bound to a single head, and 6% would have products bound to both heads. Myosin V-S1 binds to actin at 10 times the rate of either myosin V-S1-ADP or myosin V-S1-ADP-P_i (3), so it would be expected that myosin V-HMM with products bound to a single head would first bind by the rigor head and that the observed rate of product dissociation from the lead head would predominantly be from molecules in which no nucleotide was bound to the trail head. The fluorescence signal would be the result of product dissociation from the lead head. The observed rates of deac-aminoADP dissociation were fit by a single exponential of 0.006 s^{-1} (Fig. 2*F*).

Dissociation of ADP from the Actomyosin V-HMM-ADP-P_i Complex—The rapid and tight binding of deac-aminonucleotides, together with the 20-fold increase in fluorescence when bound to myosin V, make them ideal for chase experiments to determine the kinetics of ADP and P_i dissociation from actomyosin-ADP-P_i (16). In these experiments, the kinetics of dissociation of the native product, ADP, are measured, and the modified nucleotides are only used as chases to provide a fluorescent signal. We have carried out double-mixing stopped-flow experiments using similar conditions as in Fig. 2, except that ATP was used as a substrate and 22 μM deac-aminoADP or deac-aminoATP were used as chases in the presence of actin. Biphasic kinetics with fast (8.3 s^{-1}) and slow (0.041 s^{-1}) phases

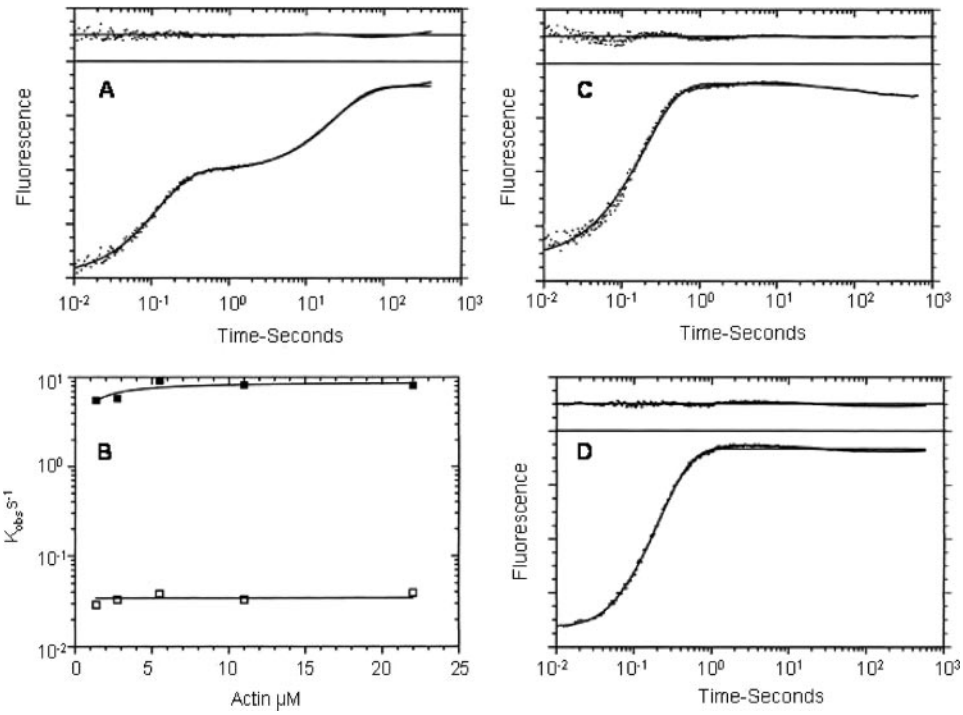

FIGURE 3. **Kinetics of product dissociation from actomyosin V-HMM-ADP-P_i.** *A*, 0.5 μM myosin V-HMM was mixed with 1.5 μM ATP, aged for 20 s, and then mixed with 20 μM actin and 40 μM deac-aminoADP. The *solid line* though the data is a fit curve of $I(t) = 0.195(1 - e^{-8.3t}) + 0.157(1 - e^{-0.041t}) + C$. *B*, actin dependence of the slow and fast rates of dissociation of ADP from actomyosin V-HMM. The experiments were similar to those in *A*, except that the actin concentrations were varied as indicated. The *lines* through the data are 8.9 s^{-1} for the fast phase and 0.035 s^{-1} for the slow phase. *C*, 0.5 μM myosin V-S1 was mixed with 1.5 μM ATP, aged for 20 s, and then mixed with 20 μM actin and 40 μM deac-aminoADP. The *solid line* though the data is a fit curve of $I(t) = 0.285(1 - e^{-8.7t} - 0.15e^{-0.48t}) + C$. *D*, 0.5 μM myosin V-HMM was mixed with 1.5 μM ATP and aged for 20 s and then mixed with 20 μM actin and 40 μM deac-aminoATP. The *solid line* though the data is a fit curve of $I(t) = 0.358(1 - e^{-5.0t} - 0.048e^{-0.0075t}) + C$.

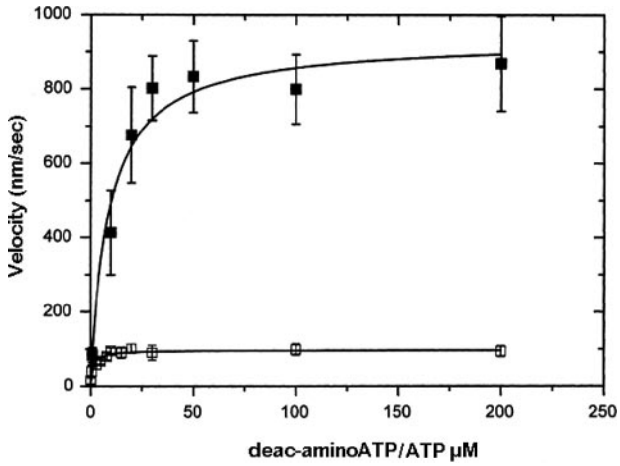

FIGURE 4. **Substrate dependence of the processive movement of myosin V-HMM.** Dependence of the velocity of myosin V-HMM movement on ATP (■) and deac-aminoATP concentrations (□) was measured with single molecule motility assay using TIRF. Data are fit to a hyperbola with a V_{max} of 920 ± 30 nm/s and a K_{app} of 8.5 ± 1.6 μM for ATP and a V_{max} of 98 ± 8 nm/s and a K_{app} of 1.3 ± 0.6 μM for deac-aminoATP.

were observed with a deac-aminoADP chase (Fig. 3*A*). The rate reached a maximum above 5 μM actin with fits of 8.9 ± 0.3 and 0.035 ± 0.005 s^{-1} over the range of actin concentrations (Fig. 3*B*). By contrast, the dissociation kinetics were >85% single exponential when myosin V-S1 was first mixed with ATP and followed by actin plus either a deac-aminoADP (Fig. 3*C*) or deac-aminoATP chase (not shown). The rate constant was 8.7 s^{-1}, similar to the fast phase observed in Fig. 3*A*. If myosin V-HMM was first mixed with ATP followed by mixing with actin plus a deac-aminoATP chase, the observed kinetics of ADP dissociation (measured by deac-aminoADP binding) was >95% monophasic with a rate constant of 5.0 s^{-1} (Fig. 3*D*).

The interpretation of these results is similar to the interpretation of those with deac-aminoATP as a substrate. For a deac-aminoADP chase with myosin V-HMM, the rapid rate of 8.9 s^{-1} is a measure of ADP dissociation from the first head, which occurs at the same rate as from actomyosin V-S1-ADP-P_i. Following the power stroke, the rate of dissociation of ADP from the second head is ~250-fold slower, 0.035 s^{-1}. With a deac-aminoATP chase, the observed rate of 4.9 s^{-1} is that expected from two sequential reactions, which were each 8.9 s^{-1}. Although the rate of the fast phase of diphosphate dissociation is 18-fold slower for deac-aminoADP (0.48 s^{-1}) than for ADP (8.9 s^{-1}), the rate of the slow phase of deac-aminoADP dissociation from the second head is only ~2-fold slower (0.015 s^{-1}) relative to ADP (0.035 s^{-1}). These results indicate that the slower dissociation rate of deac-aminoADP from the lead head measured in Fig. 2*A* is not due to the slower rate of deac-aminoADP dissociation but rather to a strain-induced change in the conformation of the myosin that reduces the rates of both ADP and deac-aminoADP dissociation. It should be noted that a low amplitude slow phase at 0.03 s^{-1} was also observed when using mdATP as the substrate with either ADP or no chase in Fig. 1.

Single Molecule Motility Assay—TIRF assays were conducted using 0.1 nM myosin V-HMM, in which the endogenous calmodulin was exchanged to Cy3-calmodulin. Although processive movement of myosin V-HMM on actin was observed from 1 to 200 μM deac-aminoATP or ATP, the length of the actin filaments prevented a quantitative comparison of run lengths between ATP and deac-aminoATP. With deac-aminoATP, a maximum velocity of 98 ± 8 nm/s and a K_{app} of 1.3 ± 0.6 μM were measured. The maximum velocity is ~10-fold less than that measured with ATP (920 ± 4 nm/s for maximum velocity and 8.5 ± 1.6 μM for K_{app}) (Fig. 4). The slower rate of motility observed with deac-aminoATP relative to ATP is in reasonably good agreement with 20-fold slower rates of dissociation of deacADP than ADP from the trail head of actomyosin V-HMM in Figs. 2

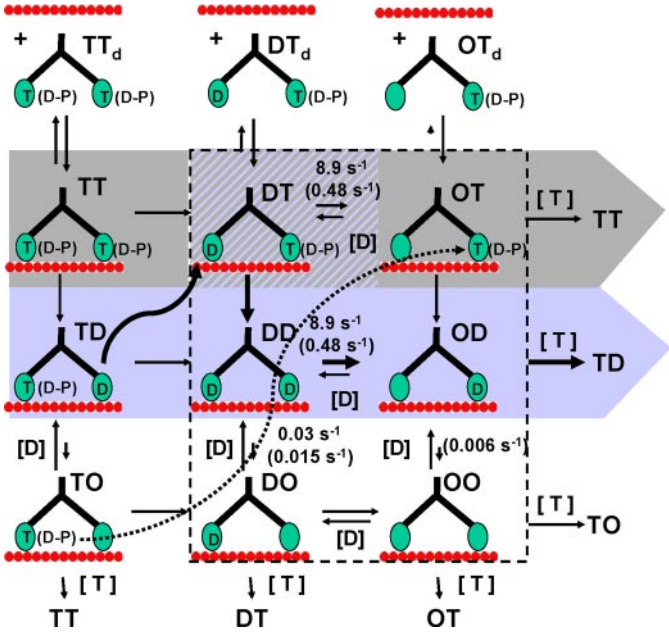

FIGURE 5. **Major actin-bound intermediates during the hydrolysis of ATP by actomyosin V.** Actomyosin V-HMM intermediates are identified by nucleotide bound to the active site. *T*, ATP or ADP-P_i; *D*, ADP; *O*, apo. Bound ATP (*T*) is assumed to be in rapid equilibrium with the hydrolysis products ADP and P_i (*D-P*). The *left-* and *right-hand letters* denote the nucleotide bound to the trail and lead heads, respectively, in the direction of movement. For example, DT has ADP bound to the trail head and ATP (or ADP-P_i) bound to the lead head, and OD has an empty trail head with a lead head containing ADP. Intermediates with the subscript *d*, (*e.g.* TT_d) are myosin V not bound to actin. Entry into the scheme in stopped-flow experiments occurs upon mixing TT_d or OT_d with actin. Alternative pathways for a single cycle of hydrolysis from TT (*upper left*) to TD (*middle right*) are in the order of predominance: *purple* > *gray* > *white* (*unshaded*). Intermediate TD (*hatched*) is common to both *purple* and *gray* pathways. The *arrows* between TO → OT and TD → DT indicate a step along the actin filament. The rate constants are for the dissociation of ADP and deac-aminoADP (in *parenthesis*) from the indicated intermediates.

and 3 and for the rates of dissociation of deac-aminoADP and ADP from the actomyosin V-S1 complex (16). These results support mechanisms in which the rate of ADP dissociation from the trail head limits the rate of processive movement by myosin V on actin.

DISCUSSION

The schematic diagram of the mechanism of ATP hydrolysis by actomyosin V in Fig. 5 contains 12 intermediates with both heads bound, 21 equilibrium constants, and 42 rate constants. Although it is a formidable, if not impossible, task to determine all of these rate and equilibrium constants unambiguously, it is important that we have a sufficient understanding of the predominant pathways to determine the mechanism by which processivity is produced and terminated. We have used double-mixing stopped-flow experiments to determine the rates of ADP and deac-aminoADP dissociation from the actomyosin V-HMM-deac-aminoADP-P_i and actomyosin V-HMM-ADP-P_i complexes. These experiments were designed to measure the rate constants of nucleoside diphosphate dissociation from the trail and lead heads of myosin V following the power stroke. The first mix of either deacATP or ATP and myosin V generates the intermediate TT_d (Fig. 5, *top left*) with either deacADP or ADP and P_i bound to both active sites. The second mix initially forms TT, and then two potential pathways lead to the formation of intermediate DT (ADP on the trail head and ATP or ADP plus P_i on the lead head). This can occur either by dissociation of P_i from the trail head (TT → DT) or from the lead head followed by a forward step (TT → TD → DT). By either route, DT has the same biochemical properties, apart from occupying a different position along the actin filament. Dissociation rates of ADP and deac-aminoADP measured here are shown in the *dashed box* in Fig. 5.

We can now consider these potential pathways for processive cycling of myosin V in terms of the scheme in Fig. 5 and how the rate constants determined here can be used to test such pathways in terms of processivity. In the mechanism proposed by Vale (25), the principal kinetic pathway is rapid dissociation of P_i from the lead head, followed by rate-limiting dissociation of ADP from the trail head and then rapid binding of ATP to the trail head. This is illustrated as the *purple path* in Fig. 5 (*i.e.* DT → DD → OD → TD → DT). Implicit in the mechanism is that slow dissociation of ADP from the lead head prevents formation of a nucleotide-free intermediate, OO, that could rapidly bind ATP to form TT, leading to dissociation of myosin V (TT_d) from actin. Rosenfeld and Sweeney (7) proposed a mechanism in which DT partitions into pathways controlled by $k_{DT\rightarrow DD}$ and $k_{DT\rightarrow OT}$. Such partitioning results in pathways that either proceed via the Vale mechanism (DT → DD → OD → TD → DT), to produce a step without dissociating from actin, or by the pathway DT → OT → TT → TT_d, which would potentially lead to dissociation and termination of a processive run.

The slow dissociation of ADP from the lead head of the actomyosin V-HMM-ADP-P_i complex following the power stroke limits the rate of ATP binding to the lead head to be 250-fold slower than to the trail head. Futile cycles in which ATP binds to an empty lead head, DO, following ADP dissociation will therefore be extremely rare events.

Rigor actomyosin V, OO, with both trail and lead heads empty of substrate or product is formed by dissociation of ADP from DO and is a potential pathway for termination of processive motion if both rigor heads rapidly bind ATP. However, partition of intermediate OD between TD and OO will favor TD by the ratio of the rates of ATP binding and ADP dissociation (*i.e.* 10^6 M^{-1} s^{-1}[ATP]/0.006 s^{-1}). Therefore, the rate of dissociation of ADP from the lead head, OD, to produce the rigor actomyosin V-HMM, OO, will be a very rare event compared with the rapid ATP binding to the empty site to produce intermediate TD, even at low concentrations of ATP.

We have observed a 2-fold larger rate for the slow component of deac-aminoADP dissociation in experiments utilizing an ADP chase compared with those in which a chase was not used (Fig. 2, *E* and *F*). These data indicate that the rate of deac-aminoADP dissociation from the lead head is increased by ADP bound to the trail head and suggests that there is increased strain on the lead head if no nucleotide is bound to the trail head. Such an effect would be expected, since it has been previously shown by single molecule mechanical studies that the myosin V has a two-step power stroke (5, 11, 12). The first 15–20 nm of the power stroke is associated with phosphate dissociation, and the second, 5 nm, occurs after the dissociation of ADP. The strain transmitted to the lead head would be

expected to depend upon the geometry of the trail head, which changes upon the dissociation of ADP. The data in Fig. 2, *C* and *D*, show that the fast fluorescence signal (from the trail head) is faster and has a smaller amplitude in the absence of a chase, but the slow fluorescence signal (from the lead head) was slower and its amplitude was unchanged in the absence of an ADP chase. These results indicate that the affinity of the deac-aminoADP for the lead head is weaker than for the trail head. Because the rate of deac-aminoADP dissociation from the lead head is 30-fold less than from the trail head, the rate of deac-aminoADP binding must be decreased by more than 30-fold to account for the lower affinity. If the rate of deac-aminoADP binding is decreased more than 30-fold, it is also highly likely that the rate of the binding of the triphosphate substrates will also be decreased by strain on the lead head. These results suggest a complementary mechanism by which strain on the lead head of myosin V-HMM-ADP decreases the rates both of ADP dissociation from and of ATP binding to the lead head. Both processes would work to increase processivity.

Although the predominant kinetic pathway is via states DT → DD → OD → TD at saturating ATP concentration, partitioning of intermediate DT between intermediates DD and OT will lead to TT. In this intermediate, ADP and phosphate are bound to both heads on the average of once every 20 catalytic cycles or steps if the rate of phosphate dissociation from both heads is at least 20-fold faster than the rate of ADP dissociation from the lead head (7). Such an intermediate would be likely to dissociate to give TT_d and terminate processive movement on average after 1.4 s ($0.69 \times 20/10\ s^{-1}$) or a distance of ~0.7 μm (20×36 nm). This is in reasonably good agreement with observed rates of dissociation of myosin V from and distances of processive movement of myosin V on actin (26, 27).

When deac-aminoATP was used as the substrate with an ADP chase, deac-aminoADP dissociation was fit by two rate constants. The more rapid ($0.48\ s^{-1}$) is attributed to deac-aminoADP dissociation from the trail head (DD → OD), which is the same as the equivalent rate for myosin V-S1. A much slower rate of $0.015\ s^{-1}$ is attributed to deac-aminoADP dissociation from the lead head; in this case, the nucleotide state of the trail head is determined by the chase nucleotide, since that head has already exchanged nucleotides. We also determined the rates of ADP dissociation from the trail head ($8.9\ s^{-1}$) and the lead head ($0.035\ s^{-1}$) using ATP as the substrate with a deac-aminoADP chase. The observed rates of dissociation of ADP and deac-aminoADP from the trail head are identical within experimental error to the rates of ADP and deac-aminoADP dissociation from actomyosin V-S1 and indicate that strain on the trail from the lead head does not significantly affect the rate of product release from the trail head (compared with unstrained myosin V-S1). These kinetic measurements are consistent with electron microscopy observations, which show a pronounced difference between the two heads in the orientation of the light chain domains during steady state ATP hydrolysis (28). The orientation of the light chain domain in the trail head is similar to that of rigor actomyosin-S1, whereas there is a 75° difference in the angle at which the light chain domain is oriented relative to the catalytic domain in the lead head. Single molecule measurements of the force dependence of ADP dissociation from single-headed myosin V-S1 predict an increase of up to 2-fold on the rate of ADP dissociation from the trail head (11, 12). The kinetic data shown here can be compared with those of Rosenfeld and Sweeney (7), who measured the rate of mdADP dissociation after binding myosin V-HMM-mdADP to actin in single mixing experiments and obtained 26 and $0.3\ s^{-1}$. However, they did not utilize ADP chase experiments to measure the rate of nucleoside diphosphate dissociation from actomyosin V-ADP-P_i following the power stroke. A fluorescence decrease at a rate, $0.03\ s^{-1}$, similar to that for ADP release from the lead head (using a deac-aminoADP chase in Fig. 3*A*) was also measured in Fig. 1 when mdATP was used as a substrate (*i.e.* following a power stroke). This can be compared with the rate of $0.3\ s^{-1}$ for the slow phase of mdADP dissociation from actomyosin V-HMM-mdADP in single mixing experiments (7). The difference between the kinetics of nucleoside diphosphate dissociation observed from actomyosin V-ADP and actomyosin V-ADP-P_i indicates that product dissociation following myosin V-HMM-ADP binding to actin does not proceed via the same intermediates as those that occur following myosin V-HMM-ADP-P_i binding to actin.

Alternative mechanisms have been proposed by Baker *et al.* and by De La Cruz (26, 28) in which the lead head, containing bound ADP and P_i, only interacts weakly with actin. In this model, the power stroke on the lead head (following P_i dissociation) is retarded until after ADP dissociation from the trail head has allowed ATP binding to that head and released the strain between the heads, as is shown by the *second row* of intermediates in Fig. 5 (TT → DT → OT). For this pathway to be significantly populated, the rate constants of P_i dissociation from DT and/or OT would have to be slow. Such slow dissociation of P_i could also provide an explanation for the slower rates of ADP dissociation from the lead head that are observed in double mixing experiments reported here compared with the more rapid rates of mdADP dissociation from actomyosin HMM measured by Rosenfeld and Sweeney (7). The slow rates of ADP, $0.035\ s^{-1}$, and deac-aminoADP dissociation, $0.015\ s^{-1}$, from actomyosin V-HMM in Figs. 2 and 3 are similar to the steady state hydrolysis rates in the absence of actin and would be consistent with a mechanism in which there is little or no activation of P_i dissociation from the lead head. In this case, the slow phase of deac-aminoADP and ADP dissociation would be limited by the P_i release at this head, rather than as a result of strain.

This interpretation of the data is not unequivocal, since a single turnover of deac-aminoATP hydrolysis, $0.027\ s^{-1}$, is faster than a single turnover of ATP hydrolysis, $0.015\ s^{-1}$, whereas the rate of deac-aminoADP release from the lead head is slower than that of ADP, and changes in the nucleotide structure may cause minor changes throughout the ATPase mechanism. In addition, the observed rate of deac-aminoADP dissociation from the lead head, measured under conditions in which the trail head does not have bound ADP ($0.006\ s^{-1}$ in Fig. 2*E*) is slower than the rate of phosphate dissociation from myosin V-deac-aminoADP-P_i in the absence of actin, $0.027\ s^{-1}$. Although not impossible, it is unprecedented for actin binding to myosin to decrease the rate of product dissociation. Single molecule mechanical experiments found that the system

dwelled in a high stiffness state with intervening periods of reduced stiffness, indicating that myosin V alternates between having one of two heads bound with high affinity (5). Recent measurements of the movement of the lead head using a gold nanoparticle-labeled calmodulin on myosin V indicate that the lead head of myosin V rotates freely about the lever arm junction before being rigidly attached with a rate constant that is similar to that determined for phosphate dissociation from actomyosin V-ADP-P_i (29). These data firmly suggest that the lead head is strongly bound to actin during a significant fraction of the kinetic cycle. We have also confirmed the measurement of Rosenfeld and Sweeney (7) of fast phosphate dissociation from both heads of actomyosin V-HMM-ADP-P_i using a fluorescent phosphate-binding protein (data not shown), which is inconsistent with models in which only one head of myosin V can be strongly attached to actin at given time. Additional evidence consistent with fast phosphate dissociation is the amplitude of the fast fluorescent signals when using mdATP as the substrate in Fig. 1, which is the same as previously observed with myosin V-S1 and by oxygen exchange measurements, which support a mechanism of rapid phosphate dissociation from both heads (30). We therefore conclude that the kinetic data support a model in which strain alters the rate of ADP dissociation following the power stroke in preference to a model in which slow P_i dissociation limits the rate of ADP dissociation.

REFERENCES

1. Wu, X. F., Bowers, B., Wei, Q., Kocher, B., and Hammer, J. A. (1997) *J. Cell Sci.* **110,** 847–859
2. Mehta, A. D., Rock, R. S., Rief, M., Spudich, J. A., Mooseker, M. S., and Cheney, R. E. (1999) *Nature* **400,** 590–593
3. De La Cruz, E. M., Wells, A. L., Rosenfeld, S. S., Ostap, E. M., and Sweeney, H. L. (1999) *Proc. Natl. Acad. Sci. U. S. A.* **96,** 13726–13731
4. Trybus, K. M., Krementsova, E., and Freyzon, Y. (1999) *J. Biol. Chem.* **274,** 27448–27456
5. Veigel, C., Wang, F., Bartoo, M. L., Sellers, J. A., and Molloy, J. E. (2002) *Nat. Cell Biol.* **4,** 59–65
6. Rief, M., Rock, R. S., Mehta, A. D., Mooseker, M. S., Cheney, R. E., and Spudich, J. A. (2000) *Proc. Natl. Acad. Sci. U. S. A.* **97,** 9482–9486
7. Rosenfeld, S. S., and Sweeney, H. L. (2004) *J. Biol. Chem.* **279,** 40100–40111
8. Purcell, T. J., Morris, C., Spudich, J. A., and Sweeney, H. L. (2002) *Proc. Natl. Acad. Sci. U. S. A.* **99,** 14159–14164
9. Walker, M. L., Burgess, S. A., Sellers, J. R., Wang, F., Hammer, J. A., Trinick, J., and Knight, P. J. (2000) *Nature* **405,** 804–807
10. Burgess, S. A., Walker, M. L., Wang, F., Sellers, J. R., Knight, P. J., and Trinick, J. (2002) *Biophys. J.* **82,** 15 (abstr.)
11. Veigel, C., Schmitz, S., Wang, F., and Sellers, J. R. (2005) *Nat. Cell Biol.* **7,** 861–869
12. Purcell, T. J., Spudich, J. A., and Sweeney, H. L. (2005) *Proc. Natl. Acad. Sci. U. S. A.* **102,** 13873–13878
13. Steffen, W., Smith, D., and Sleep, J. (2003) *Proc. Natl. Acad. Sci. U. S. A.* **100,** 6434–6439
14. Smith, D. A., and Sleep, J. (2004) *Biophys. J.* **87,** 442–456
15. White, H. D., Cartwright, S. L., Wang, F., and Sellers, R. J. (2003) *Biophys. J.* **84,** 116 (abstr.)
16. Forgacs, E., Cartwright, S., Kovács, M., Sakamoto, T., Sellers, J. R., Corrie, J. E. T., Webb, M. R., and White, H. D. (2006) *Biochemistry* **45,** 13035–13045
17. Wang, F., Chen, L. F., Arcucci, O., Harvey, E. V., Bowers, B., Xu, Y. H., Hammer, J. A., and Sellers, J. R. (2000) *J. Biol. Chem.* **275,** 4329–4335
18. Gill, S., and von Hippel, P. (1989) *Anal. Biochem.* **182,** 319–326
19. Spudich, J. A., and Watt, S. (1971) *J. Biol. Chem.* **246,** 4866–4871
20. Hiratsuka, T. (1983) *Biochim. Biophys. Acta* **742,** 496–508
21. Webb, M. R., Reid, G. P., Munasinghe, V. R. N., and Corrie, J. E. T. (2004) *Biochemistry* **43,** 14463–14471
22. Sakamoto, T., Wang, F., Schmitz, S., Xu, Y. H., Xu, Q., Molloy, J. E., Veigel, C., and Sellers, J. R. (2003) *J. Biol. Chem.* **278,** 29201–29207
23. Eccleston, J. F., Hutchinson, J. P., and White, H. D. (2001) in *Protein-Ligand Interactions: Structure and Spectroscopy* (Harding S. E., and Chowdhry, B. Z., eds) pp. 201–237, Oxford University Press, Oxford
24. Cremo, C. R., Wang, F., Facemyer, K., and Sellers, J. R. (2001) *J. Biol. Chem.* **276,** 41465–41472
25. Vale, R. (2003) *J. Cell Biol.* **163,** 445–450
26. Baker, J. E., Krementsova, E. B., Kennedy, G. G., Armstrong, A., Trybus K. M., and Warshaw, D. M. (2004) *Proc. Natl. Acad. Sci. U. S. A.* **101,** 5542–5546
27. Sakamoto, T., Yildiz, A., Selvin, P. R., and Sellers, J. R. (2005) *Biochemistry* **44,** 16203–16210
28. De La Cruz, E. M., and Ostap, E. M. (2004) *Curr. Opin. Cell Biol.* **16,** 61–67
29. Dunn, A. R., and Spudich, J. A. (2007) *Nat. Struct. Mol. Biol.* **14,** 246–248
30. Olivares, A. O., Chang, W., Mooseker, M. S., Hackney, D. D., De La Cruz, E. M. (2006) *J. Biol. Chem.* **281,** 31326–31336